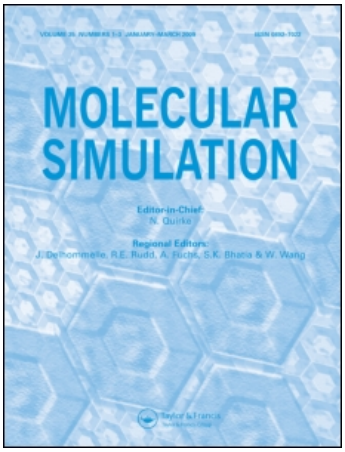

Molecular Simulation

Publication details, including instructions for authors and subscription information:
http://www.informaworld.com/smpp/title~content=t713644482

Replica-exchange molecular dynamics simulation of diffracted X-ray tracking

Y. Kawashima[ab]; Y. C. Sasaki[ac]; Y. Sugita[d]; T. Yoda[e]; Y. Okamoto[ab]

[a] CREST-Sasaki Team, Japan Science and Technology Agency (JST), Tachikawa, Tokyo, Japan [b] Department of Physics, School of Science, Nagoya University Furo-cho, Nagoya, Aichi, Japan [c] JASRI/SPring-8, Mikazuki, Hyogo, Japan [d] Institute of Molecular and Cellular Biosciences, University of Tokyo, Bunkyo-ku, Tokyo, Japan [e] Nagahama Institute of Bio-Science and Technology, Nagahama, Shiga, Japan

To cite this Article Kawashima, Y. , Sasaki, Y. C. , Sugita, Y. , Yoda, T. and Okamoto, Y.(2007) 'Replica-exchange molecular dynamics simulation of diffracted X-ray tracking', Molecular Simulation, 33: 1, 97 — 102
To link to this Article: DOI: 10.1080/08927020601067581
URL: http://dx.doi.org/10.1080/08927020601067581

Molecular Simulation, Vol. 33, Nos. 1–2, 15 January–15 February 2007, 97–102

Taylor & Francis
Taylor & Francis Group

Replica-exchange molecular dynamics simulation of diffracted X-ray tracking

Y. KAWASHIMA†‡*, Y. C. SASAKI†¶, Y. SUGITA§, T. YODA‖ and Y. OKAMOTO†‡

†CREST-Sasaki Team, Japan Science and Technology Agency (JST), Tachikawa, Tokyo 190-0012, Japan
‡Department of Physics, School of Science, Nagoya University Furo-cho, Chikusa-ku, Nagoya, Aichi 464-8602, Japan
¶JASRI/SPring-8, Mikazuki, Hyogo 679-5198, Japan
§Institute of Molecular and Cellular Biosciences, University of Tokyo, Yayoi, Bunkyo-ku, Tokyo 113-0032, Japan
‖Nagahama Institute of Bio-Science and Technology, Tamura, Nagahama, Shiga 526-0829, Japan

(Received 15 October 2006; in final form 16 October 2006)

We examine the effects of the nanocrystal covalently bonded to one end, utilizing replica-exchange molecular dynamics simulation of a peptide with the sequence Ac-YGKAAAAKAAAAKAAAAKC-amide, to simulate the diffraction X-ray tracking (DXT) method. We performed three different simulations in this study. A simulation with no constraint, a simulation with one end fixed, and a simulation with one end fixed and also considering the effect of the nanocrystal by changing the mass of the sulfur atom in the C-terminus, which covalently bonded with the Au nanocrystal in diffraction DXT method, was performed. The average configuration parameters of the three simulations are compared and discussed. We analyzed our simulation results utilizing principal component analysis. The obtained free-energy landscape indicated that the condition of the DXT technique will not affect the global-minimum state, however, it may affect the folding pathway.

Keywords: Generalized-ensemble algorithm; REMD; Diffracted X-ray tracking; DXT

1. Introduction

Continuous effort has been made to measure the dynamic structural information of single-biomolecules and effective methods have been developed [1–3]. One of the methods, single molecular imaging with laser-induced fluorescence, realizes measurements of molecular dynamics in physiological environment. However, the wavelength of the light in the visual region limits the accuracy of the positional information [3]. Thus, detecting the conformational change of single molecule is difficult. On the other hand, diffracted X-ray tracking (DXT) [1] enables us to measure single molecule dynamics in accuracy of picometer level. DXT has been applied to DNA molecules [1,4] and bacteriorhodopsin single molecules [5] and succeeded in tracking the single-molecule motion with high accuracy. However, the microscopic configuration information of the all-atom model will help understanding the data further.

In our previous study [6], we employed all-atom molecular dynamics simulation to discuss the microscopic features of the biomolecule. Simulating biomolecules and obtaining good ensemble is a difficult task, since employing the potential energy functions available for all-atom models leads to the trapping of the trajectories in the local-minimum states, which exists in large numbers in biomolecular systems. In order to overcome the local-minimum states, we introduced the replica-exchange molecular dynamics (REMD) method [7], one of the powerful generalized-ensemble techniques [8,9].

We studied the effect of one end of the biomolecule fixed to the substrate in single-molecule imaging techniques. Since the biomolecules observed in the single-molecule imaging techniques are fixed to different conditions from the biomolecules *in vivo*, we needed to elucidate the effect of the fixed end. A small peptide YG found in their literature [10], which has a stable α-helix in water among the alanine-based peptides, is applied to all-atom simulations based on REMD. We found that the peptide motion with one end fixed was slightly limited compared to the peptide which was not fixed.

In this work, we also study the effect of the heavy nanocrystal covalently bonded to the biomolecule by REMD. Because we are interested in the microscopic

*Corresponding author. Email: snow@tb.phys.nagoya-u.ac.jp

Molecular Simulation
ISSN 0892-7022 print/ISSN 1029-0435 online © 2007 Taylor & Francis
http://www.tandf.co.uk/journals
DOI: 10.1080/08927020601067581

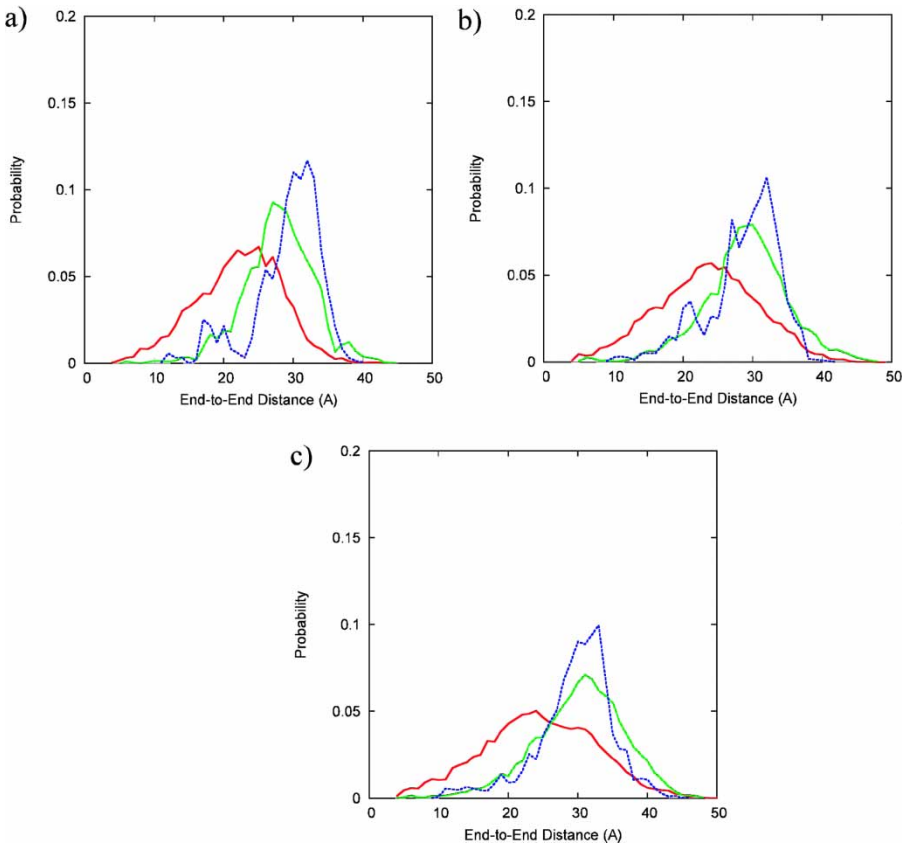

Figure 1. Histograms of end-to-end distance: (a) 297 K, (b) 405 K and (c) 504 K. The red, green and blue lines correspond to the "Free", "Fixed" and "Fixed + Heavy" simulations, respectively (colour in online version).

feature of the biomolecule only, the nanocrystal is not treated explicitly. The nanocrystal is very large compared to atoms, and in DXT [1], it shows Brownian motion which is in a different scale with the atoms in biomolecules. Thus, we approximate the effect of the nanocrystal by changing the mass of the sulfur atom in the C-terminus Cysteine, which is directly bonded with the nanocrystal in DXT. Three simulations in different conditions were carried out. First, we simulated the system without any constraints. Then, we simulated the system with one end fixed. Finally, we performed simulation with one end fixed and the other end having a heavy sulfur atom. The results of our simulations and the comparison among the three simulations are made with the free energy landscapes obtained.

2. Methods

REMD [7] method, was applied to a peptide Ace-YGKAAAAKAAAAKAAAAKC-amide. Cys residue is added to the peptide original YG (Ace-YGKAAAAKA-AAAKAAAAK-amide) in Ref. [10], because the sulfur atom of Cys residue is used to form a covalent bond with the nanocrystal in DXT [1]. CHARMM22 all-atom force field [11] and TIP3P [12] model was used for the peptide and rigid water molecules, respectively. Yoda *et al.* [13,14] reported that CHARMM22 works well with systems which have α-helix structures. For REMD, 48 temperatures between 250 and 700 K (250, 255, 261, 267, 273, 279, 285, 291, 297, 304, 311, 318, 325, 332, 339, 347, 355, 363, 371, 379, 387, 396, 405, 414, 423, 432, 442, 452, 462, 472, 482, 493, 504, 515, 526, 538, 550, 562, 538, 550, 562, 574, 587, 600, 613, 627, 641, 655, 670, 685, 700) were used. For further details, see Ref. [8].

Three different simulations were performed. The first simulation was carried out without any constraints (referred to as "Free", hereafter). The second simulation had the carbonyl carbon in Ace fixed (referred to as "Fixed", hereafter). In the DXT method, the N-termius is linked to the substrate. Thus, we fixed the first atom connected to the N-terminus of the peptide. In the DXT method, the sulfur atom is also covalently bonded to a nanocrystal. The final simulation thus had the carbonyl carbon in Ace fixed, and the mass of the sulfur atom in Cys was set tobe 229.0260, heavier than the normal value of 32.0600, to mimic the effect of the heavy nanocrystal (referred to as "Fixed + Heavy", hereafter). In spite of the change of mass, the potential parameters were not changed. To keep the HS bond of cysteine stable, LINCS algorithm [15] was applied to the HS bond. All simulations started from 20 ps of canonical run, followed by 2.2 ns (per replica) of REMD run. Replica exchange trial was made at every 10 fs. The peptide was soaked in a sphere of radius 27 Å filled with 2580 water molecules. Harmonic

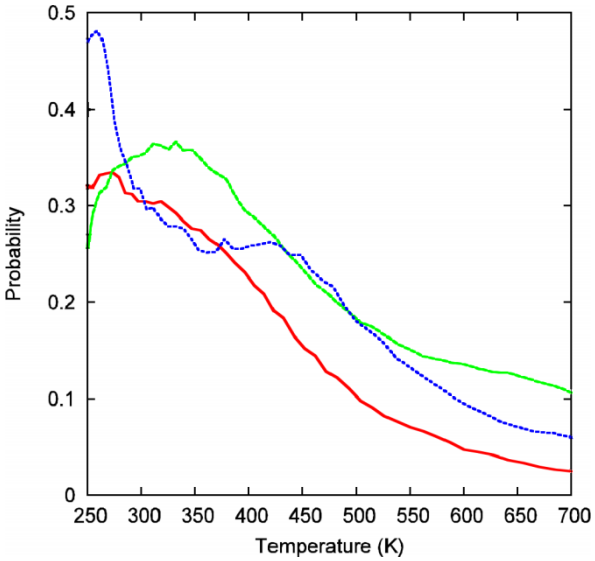

Figure 2. Average helicity as the function of temperature (K).

restraint was used to prevent water molecules and the peptide from getting out of the sphere.

All of our simulations were performed by the modified version [16,17] of PRESTO version 2 [18]. The pictures of the peptides were created by Molscript [19] and Raster3D [20].

3. Results and discussion

In DXT, the dynamics of a nanoparticle is observed. In our simulation, similar information can be obtained by monitoring the end-to-end distance of the peptide. Here, we define the end-to-end distance to be the distance from the carbonyl carbon atom of acetyl N-terminus, which is fixed in the DXT, to the sulfur atom of cysteine, which is covalently bonded in DXT. Histograms of the end-to-end distance distributions are shown in figure 1(a)–(c) correspond to the histograms at 297, 405 and 504 K, respectively. For all simulations, as the temperature increases, the range of the end-to-end distance widens. The range of the end-to-end distance for the "Fixed" simulation is delocalized compared to the "Fixed + Heavy" simulation, while it is localized compared to the "Free" simulation. By comparing the results of the "Fixed" simulation and the "Free" simulation, the effects of the fixed N-terminus can be studied, while comparing the "Fixed" simulation and the "Fixed + Heavy" simulation, the effects of the nanoparticle bonded to the sulfur near the C-terminus can be studied. The values of end-to-end distance for the "Fixed" simulation are smaller compared to the "Free" simulation in all temperatures. Comparing the results of the two simulations, both the peak of the histogram and the range of the histogram in the

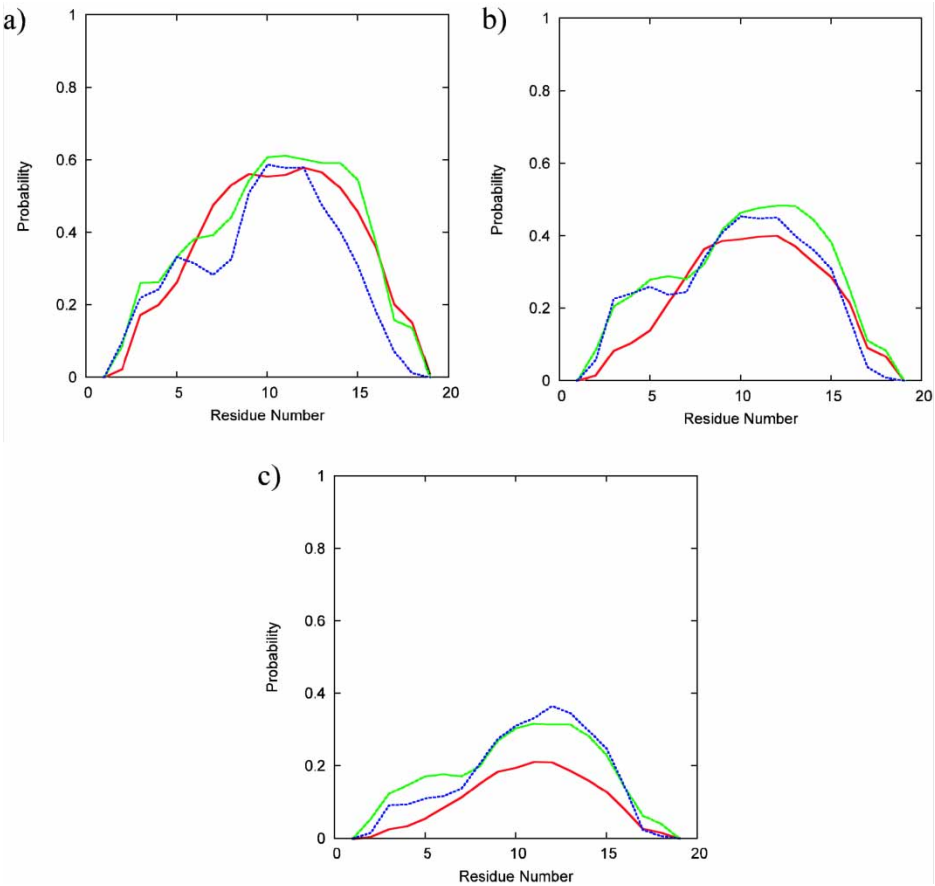

Figure 3. Histograms of helicity: (a) 297 K, (b) 405 K and (c) 504 K. The red, green and blue lines correspond to the "Free", "Fixed" and "Fixed + Heavy" simulations, respectively (colour in online version).

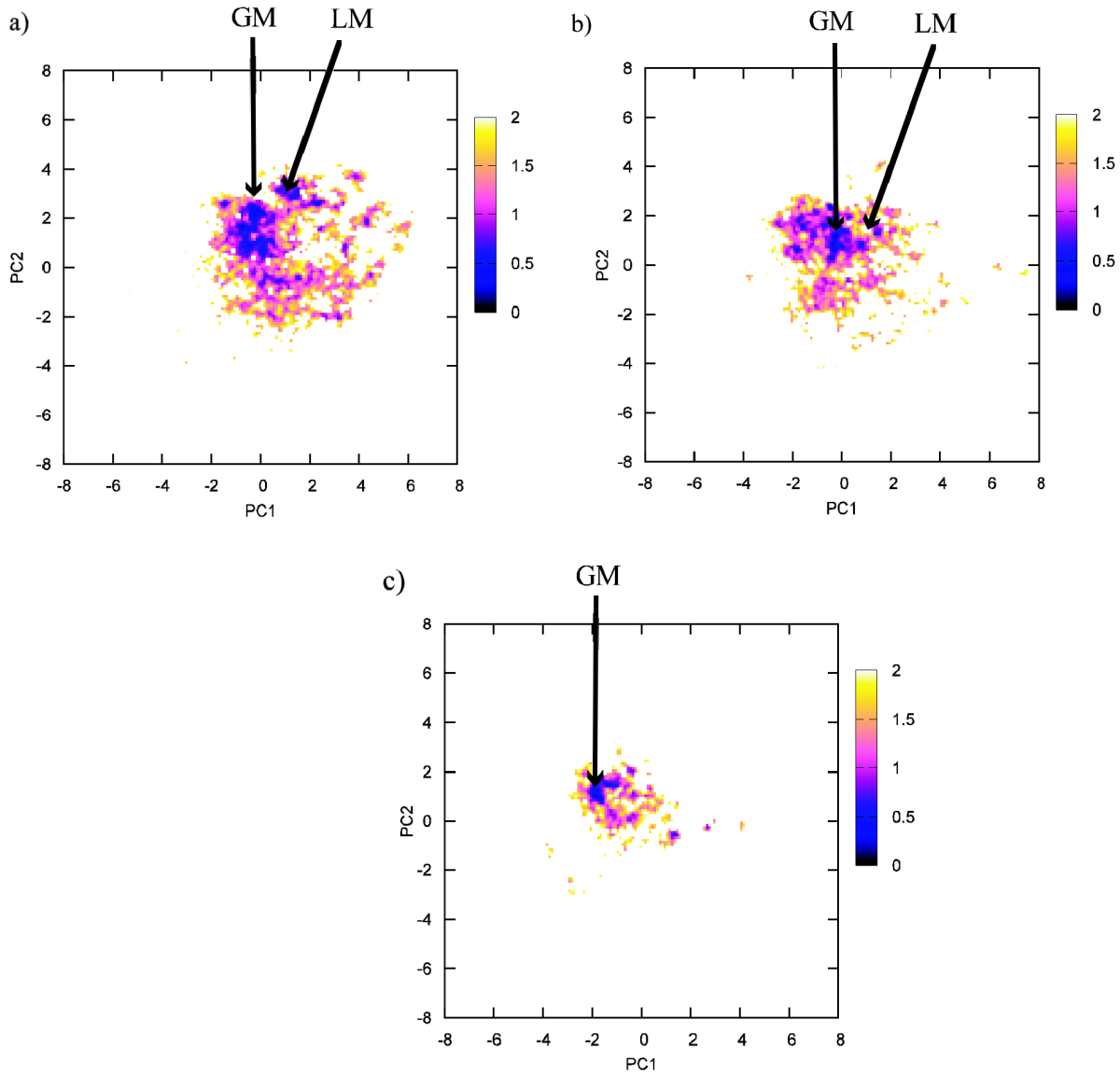

Figure 4. Potential of mean force (kcal/mol) along the two components at 297 K of: (a) "Free", (b) "Fixed" and (c) "Fixed + Heavy" simulation respectively.

"Fixed" simulation is shifted to the larger values. As in DXT experiments, the motion of the C-terminus that approaches to the N-terminus is restricted in "Fixed" and "Fixed + Heavy" simulations, while "Free" simulations are not. Hence, the peak and the range of the end-to-end distance are shifted to the smaller region in the "Free" simulation. The "Fixed + Heavy" simulation shows the same tendency as in the "Fixed" simulation. On the other hand, the range of the end-to-end distance for the "Fixed" simulation is larger compared to the "Fixed + Heavy" simulation. Especially, in the case of 297 K (figure 1(a)), most of the configurations found in the "Fixed + Heavy" simulation have the end-to-end distance in the range of 30–33 Å, which is the same range of the configurations with the complete α-helix. This shows that the heavy atom on the C-terminus side limits the motion of the peptide. At temperatures 405 and 504 K, the shape of the histogram of the "Fixed + Heavy" simulation becomes similar. This indicates that the motion of the heavy sulfur atom in the "Fixed + Heavy" simulation become large and does not affect the motion at low temperatures.

We next examine the helicity of the peptide, which is the main structural feature of this peptide to see the effects of the DXT observation condition. In figure 2, we plot the average helicity (with the number of α-helical residues in the peptide defined by DSSP [21]) as a function of temperature. "Free" and "Fixed" simulations show similar tendency. However, the configurations obtained from the "Fixed" simulation have more helical residues compared to the "Free" simulation in the high temperature region. The helices in the "Fixed" simulation are more stable than the "Free" simulation case. In our previous work, we found that the motion of the "Fixed" simulation is limited compared to the "Free" simulation, and this can explain

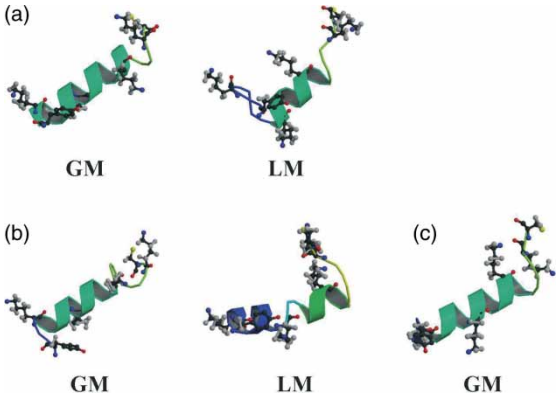

Figure 5. The representative structures at the free-energy GM -states and a stable LM states of: (a) "Free", (b) "Fixed" and (c) "Fixed + Heavy" simulation respectively.

the stability of the helices in the "Fixed" simulation. The "Fix + Heavy" simulation shows different characteristics with the other two simulations. The "Fix + Heavy" simulation seems to show a two step decrease in average helicicty as the temperature increases while the other two decreases monotonically which is the general case for helical peptides.

We have observed CD spectra for "free" Ace-YGKA-AAAKAAAAKAAAAKC-amide and nanoparticle-C-YGKAAAAKAAAAKAAAAKC-nanoparticle systems in 293 K. The CD spectra for the two systems showed no difference. The experimental results can be compared with the helicity values of the "Free" simulation and the "Fixed + Heavy" simulation in 297 K. The helicity for the "Free" simulation and the "Fixed + Heavy" simulation was 0.30 and 0.31, respectively. The helicity between the two simulation at 300 K was very similar and showed the same tendency with the experimental data.

We study further the difference of the helicity among the three simulations. Because the peptide has symmetrically distributed Lys residues, we consider the following three regions: Lys3-Lys8 (N region, hereafter), Lys8-Lys13 (M region, hereafter) and Lys13-Lys18 (C region, hereafter). In figure 3, we show histograms of the helicity for each residue at 297, 405 and 504 K, in a, b and c, respectively. For all simulations, as the temperature increases, the helicity of each residue decreases. In the case of 297 K, we compared the helicity of "Free" and "Fixed" simulations within the three regions: N, M and C regions. The difference of the helicity compared by regions was not significant [6]. However, the shape of the histogram is different. The difference of the shape between the histograms of the "Free" simulation and the "Fixed + Heavy" simulation at 297 K is significant. The shape of the "Free" simulation shows that the helix of M region is very stable compared to the other regions and as the residues become farther from the center, the helicity reduces monotonically. All of the residues in the N region of the "Fixed + Heavy" simulation have similar values. The "Fixed" simulation in 405 and 504 K shows similar tendencies with the "Fixed + heavy" simulations, which is consistent with the end-to-end distance histogram in figure 1.

For further understanding, we used principal component analysis (PCA) [22–24] to obtain the free-energy landscape. Each configuration was projected on to the first two principal axes to illustrate the free-energy landscape, which is given as the potential of mean force with principal component (PC) axes as reaction coordinates.

The potential of mean force obtained from the "Free" simulation along the first two PC axes (PC1 and PC2) is shown in figure 4. Figure 4(a)–(c) corresponds to the results of "Free", "Fixed" and "Fixed + Heavy" simulations, respectively. At 297 K, which is close to room temperature, the conformation states are localized, and a rough free-energy landscape is obtained. Along the PC1 axis, the free energy surface of the "Free" simulation has the widest range compared to the other simulations. The "Fixed" simulation has a wider range compared to the "Fixed + Heavy" simulation. The PC1 axis is correlated with the end-to-end distance (the correlation coefficient is -0.419). Hence, the range along the PC1 axis corresponds to the motion range of the end-to-end distance, and the free energy surface shows the same tendency with the histogram of the end-to-end distance in figure 1. The negative correlation coefficient indicates that the large PC1 value results to the small end-to-end distance. The free energy surface of the "Free" simulation shift to the large side of the PC1 axis, while the surface of the "Fixed + Heavy" simulation shift to the small side, compared to the "Fixed" simulation surface. This order also consists with the end-to-end histogram. The ordering for the width of the range along the PC2 axis was the same as in PC1 axis. This shows that the motion of the peptide in the "Fixed + Heavy" simulation is limited compared to the "Fixed" simulation, which is limited compared to the "Free" simulation (figure 4).

Let us compare the characteristics of the free-energy global-minimum state obtained from the three simulations. A representative snapshot of the global minimum (GM) states and local minimums (LM) are shown in figure 5. All three snapshots have a single helix conformation and have a stable helix in the M region. We next compare the LM snapshot. In the "Free" simulation, the snapshot of the LM also has a single helix conformation with a stable helix in the M region, but has a shorter helix. We must also mention that the end-to-end distance is smaller than the GM snapshot, which leads to the breaking of hydrogen-bonds. This indicates that the motion of both ends causes the decrease of the helical residues which leads to unfolding of the peptide. The snapshot of the LM found in the "Fixed" simulation has a double-helix structure. We have found many double-helix structures, while it was not found in the "Free" simulation. This indicates that unlike the "Free" simulation, in "Fixed" simulation, the motion of the C-terminus leads to the division of the helix which leads to unfolding of the peptides. And for the "Fixed +

Heavy" simulation, a stable LM was not found. This can be explained by the limitation of motion, which leads to a small fluctuation in the region of the global-minimum state. However, many two-helix structures were also found in the "Fixed + Heavy" simulation. It can be predicted that the motion of the peptide under DXT condition is similar to the motion of "Fixed" simulation. These results indicate that the DXT observation condition does not affect the GM, however, the pathway of folding and unfolding which may change for molecules which exist in solution as the peptide in this study.

4. Conclusions

In this work, we have studied the effects of fixing one end in single-molecule imaging techniques, and the effect of the nanoparticle bonded on the other end in DXT techniques by three REMD simulations at three different conditions, of a small α-helical peptide. The configuration parameters, end-to-end distance and helicity, was compared among the three simulations and discussed. Free energy landscape was obtained using the first and second PC axes obtained from PCA, which represent the backbone motion and the reorganization of the backbone hydrogen-bonds, respectively. The global-minimum states of free energy in the three simulations are similar, and have a single α-helical segment. However, the LM differed in each simulation. This indicates that the folding pathway might be affected in the case of biomolecules in solution as in this work. Since the static characters were understood, we next plan to seek the dynamics of DXT [1].

Acknowledgements

The computations were performed on the computers at the Research Center for Computational Science, Institute of Molecular Science. This work was supported, in part, by the Grants-in-Aid for the NAREGI Nanoscience Project and for Scientific Research in Priority Areas, "Water and Biomolecules", from the Ministry of Education, Culture, Sports, Science and Technology, Japan.

References

[1] Y.C. Sasaki, Y. Suzuki, N. Yagi, S. Adachi, M. Ishibashi, H. Suda, K. Toyota, M. Yanagihara. Tracking of individual nanocrystals using diffracted x rays. *Phys. Rev. E*, **62**, 3843 (2000); Y.C. Sasaki, Y. Okumura, S. Adachi, H. Suda, Y. Taniguchi, N. Yagi. Picometer-Scale Dynamical X-Ray Imaging of single DNA Molecules. Phys. Rev. Lett., 87, 248102 (2001).

[2] S. Weiss. Fluorescence spectroscopy of single biomolecules. *Science*, **283**, 1676 (1999).

[3] W.E. Moerner, M. Orrit. Illuminating single molecules in condensed matter. *Science*, **283**, 1670 (1999).

[4] Y.C. Sasaki, Y. Okumura, S. Adachi, Y. Suzuki, N. Yagi. Diffracted X-ray tracking: new system for single molecular detection with X-rays. *Nucl. Instrum. Methods Phys. Res. A*, **467**, 1049 (2001).

[5] Y. Okumura, M. Oka, Y. Kataoka, Y.C. Taniguchi. Picometer-scale dynamical observations of individual membrane proteins: the case of bacteriorhodopsin. *Phys. Rev. E*, **70**, 021917 (2004).

[6] Y. Kawashima, Y. Sugita, T. Yoda, Y. Okamoto. Effects of the fixed end in single-molecule imaging techniques: a replica-exchange molecular dynamics simulation study. *Chem. Phys. Lett.*, **414**, 449 (2005).

[7] Y. Sugita, Y. Okamoto. Replica-exchange molecular dynamics method for protein folding. *Chem. Phys. Lett.*, **314**, 141 (1999).

[8] A. Mitsutake, Y. Sugita, Y. Okamoto. Generalized-ensemble algorithms for molecular simulations of biopolymers. *Biopolymers*, **60**, 96 (2001).

[9] Y. Sugita, Y. Okamoto. Free-energy calculations in protein folding by generalized-ensemble algorithms. In *Computational Methods for Macromolecules: Challenges and Applications*, T. Schlick, H.H. Gan (Eds.), p. 304, Springer-Verlag, Berlin (2002).

[10] A. Chakrabartty, T. Kortemme, R.L. Baldwin. Helix propensities of the amino acids measured in alanine-based peptides without helix-stabilizing side-chain interactions. *Protein Sci.*, **3**, 843 (1994).

[11] A.D. MacKerrel Jr., D. Bashford, M. Bellot, R.L. Dunbrack Jr., J.D. Evanseek, M.J. Field, S. Fischer, J. Gao, H. Guo, S. Ha, D. Joseph-McCarthy, L. Kuchnir, K. Kuczera, F.T.K. Lau, C. Mattos, S. Michnick, T. Ngo, D.T. Nguyen, B. Prodhom, W.E. Reiher III, B. Roux, M. Schlenkrich, J.C. Smith, R. Stote, J. Straub, M. Watanabe, J. Wiórkiewicz-Kuczera, D. Yin, M. Karplus. All-atom empirical potentiel for molecular modeling and dynamics studies of proteins. *J. Phys. Chem. B*, **102**, 3586 (1998).

[12] W.L. Jorgensen, J. Chandrasekhar, J.D. Madura, R.W. Impey, M.L. Klein. Comparison of simple potential functions for simulating liquid water. *J. Chem. Phys.*, **79**, 926 (1983).

[13] T. Yoda, Y. Sugita, Y. Okamoto. Comparisons of force field for proteins by generalized-ensemble simulations. *Chem. Phys. Lett.*, **386**, 460 (2004).

[14] T. Yoda, Y. Sugita, Y. Okamoto. Secondary-structure preference of force fields for proteins evaluated by generalized-ensemble simulations. *Chem. Phys.*, **307**, 269 (2004).

[15] B. Hess, H. Bekker, H.J.C. Berendsen, J.G.E.M. Fraaije. LINCS: a linear constraint solver for molecular simulations. *J. Comp. Chem.*, **18**, 1463 (1997).

[16] A. Kitao, S. Hayward, N. Go. Energy landscape of a native protein: jumping-among-minima model. *Proteins*, **33**, 496 (1998).

[17] Y. Sugita, A. Kitao. Improved protein free energy calculation by more accurate treatment of nonbonded energy: application to chymotrypsin inhibitor 2, V57A. *Proteins*, **30**, 388 (1998).

[18] K. Morikami, T. Nakai, A. Kidera, M. Saito, H. Nakamura. PRESTO: a vectorized molecularmechanics program for biopolymers. *Comput. Chem.*, **16**, 243 (1992).

[19] P.J. Kraulis. MOLSCRIPT: a program to produce both detailed and schematic plots of protein structures. *J. Appl. Crystallogr.*, **24**, 946 (1991).

[20] D. Bacon, W.F. Anderson. A fast algorithm for rendering space-filling molecule pictures. *J. Mol. Graphics.*, **6**, 219 (1988); E.A. Merritt, D. Bacon. Raster3D: Photorealistic molecular graphics. Methods in Enzymology, **277**, 205 (1997).

[21] W. Kabsch, C. Sander. Dictionary of protein secondary structure: pattern recognition of hydrogenbonded and geometrical features. *Biopolymers*, **22**, 2577 (1983).

[22] A. Kitao, F. Hirata, N. Go. The effects of solvent on the conformation and the collective motions of protein: normal mode analysis and molecular dynamics simulations of melittin in water and in vacuum. *Chem. Phys.*, **158**, 447 (1991).

[23] A.E. Garcia. Large-amplitude nonlinear motions in proteins. *Phys. Rev. Lett.*, **68**, 2696 (1992).

[24] A. Amadei, A.B.M. Linssen, H.J.C. Berendensen. Essential dynamics of proteins. *Proteins*, **17**, 412 (1993).